

**Fig. 5.** Panels show the evolution of the supercell reconstructed using the GOS-TOPOENACHED model run at 10:10UTC (panels a,d,g,l), 10:20 UTC (panels b,e,h, m), 10:30UTC (panels c,f,i,n). Panels a-c show the accumulated rain, hail (contour) and storm-relative helicity (0-3000 m). The vectors represent the wind direction and speed between 750 and 500 hPa (every 50 hPa). Panels d-f show the maximum reflectivity and hail on the ground (black contours). In addition, the wind direction is shown at an altitude of 3000 m. Panels g-i show  $\theta_e$  and reflectivity (dBZ) and wind at 3000 m. Panels l-n show the absolute vorticity, reflectivity (contour) and the wind at 3000 m above sea level.

(Fig\_supp\_1), and the WRF radio sounding in the center of the storm cell are used. First, a consistent vertical profile, between observations and model results, at Zadar and Pratica di mare is observed (Fig\_supp\_1). Because of the large difference in resolution between the model (1 km) and the Cloud Top height satellite data (10 km), the two datasets are not

directly comparable, but they can communally provide important information, which confirms that the simulation produces results consistent with the observations, for such a key variable as the altitude reached by the storm. Therefore, the comparison of the two datasets is not presented between the images, but is added to the supplementary

material (Fig. suppl\_3). In Fig. suppl\_3a-c, the cloud top from SEVIRI shows the top of the troposphere at approximately 12,000–14,000 m, at 10:00, 10:15 and 10:30 UTC, similar to the values inferred from the radio soundings from Zadar and Pratica di mare at 1200 UTC (Fig. suppl\_1). During the most intense phase of the supercell, the anvil expands and deepens reaching approximately 12,500 m (Fig. suppl\_3a,c orange), and the overshooting tops reach 14,000–14,500 m (Fig. suppl\_3a-c, dark red) along the coast line. Similarly, the WRF model cloud-top anvil reaches 12,500–13,000 m (Fig. suppl\_3d-f, dark orange) and the overshooting top reaches 14,500 m (Fig. suppl\_3d,e, gray). The observed brightness (Figs. 6a,c) shows the overshooting top temperature exceeding  $-70^{\circ}\text{C}$ , whereas that from WRF reaches approximately  $-75/-78^{\circ}\text{C}$ , consistent with convection stronger in simulations than in observations. These temperature values are extremely low, indicating an intense and deep vertical motion (Figs. 6d,e). The Zadar and Pratica di Mare radio soundings (Fig. suppl\_1) show the tropopause at approximately 12,500–13,000 m and at  $T = -80^{\circ}\text{C}$ , supporting the previous hypothesis. SEVIRI also shows an area with a decrease in the cloud-top altitude (Fig. suppl\_3a-c), corresponding to the Central Warm Spot (CWS, [Setvák et al., 2010](#)), at approximately 11,500 m, i.e. the yellow area in the center of the anvil. Similarly, the WRF model produces a region with a decrease of the cloud-top height (Fig. suppl\_3e,f, orange) intruding into the anvil, on the lee side of the overshooting top. The CWS is clearly associated with a decrease of the brightness temperature both in SEVIRI and in WRF output (Figs. 6a-c and Figs. 6d-f, respectively).

Specifically, during the mature stage a large anvil reaching the top of the tropopause is observed suggesting an extensive and very intense convective activity. Downstream of the overshooting a ‘Cold Ring Shape’ ([Setvák et al., 2010](#)), enclosing a Central Warm Spot (CWS), is found. These structures are characteristic of supercells ([Setvák et al., 2010](#)). The CWS is characterized by a lower altitude of a few hundred meters and by a negative horizontal vorticity near the overshooting top. Aside from the SEVIRI temperature dropping to  $-65/70^{\circ}\text{C}$ , the overshooting top maintains its strength and altitude to break through the tropopause; WRF shows (Figs. 6a-c and Figs. 6d-f, respectively) a similar

behavior.

- Cell structure: vertical velocity,  $\Theta_e$ , reflectivity, and hydrometeors

In this section the analysis of the vertical structure of the cell simulated by WRF, at the same times used for the two-dimensional analysis, is performed. Fig. 7 shows the cross sections of the main cell (panels a,c,e,g) and along the axis joining the two cells (panels b,d,f,h) at 10:10 UTC. For easier interpretation, Fig. suppl\_2 (supplementary material) is complementary to Fig. 7 and Fig. 8, in which the vertical velocity in shaded and contour is shown. The vertical velocities (solid lines) and  $\Theta_e$  (shaded colors) show the maximum development of the cell (Fig. 7a, Fig. suppl\_2a) at 10:10 UTC. Relatively cold, dry air, arriving from the north Adriatic is found in the first 400 m of the atmosphere (right side), together with mild, humid air from the southeast, with  $\Theta_e$  values close to  $65-68^{\circ}\text{C}$  between 400 and 800 m (left side), all converging toward the cell. The cross section of the cell shows (Fig. 7a, solid lines, and Fig. suppl\_2a) vertical velocity ( $W$ ) exceeding  $20\text{ ms}^{-1}$  from 5 km to 16 km, with a maximum core of  $W$  reaching  $50\text{ ms}^{-1}$  between 10 and 13 km. Within this strong updraft  $\Theta_e$  reaches values of  $80^{\circ}\text{C}$ . The observed overshooting top (Figs. 6a-c) clearly supports this structure.

At the top of the cell, a tongue of high  $\Theta_e$  intruding downward on the east side of the cell is clearly associated with a strong downdraft area and negative vertical vorticity as shown in Figs. 7g,h. Furthermore, the updraft is surrounded by cooler air generated by the ‘‘evaporational cooling’’ effect as suggested by the lower value of  $\Theta_e$  (Fig. 7a) between 10 and 14 km. On the east side of the cell a downdraft with a vertical velocity of  $-10\text{ ms}^{-1}$  is found, between 4 and 10 km (Fig. 7a and Fig. suppl\_2a). In the first 5 km, the updraft is slightly tilted along the direction of propagation (Figs. 7a,c,d) and in the same layers there is a colder and drier area - the Rear Flank Downdraft (RFD) - generated by precipitation. The associated downdraft and the RFD are clearly shown by the radar reflectivity and the vertical velocity (Fig. 7c, the blue area, and Fig. 7d, the white area). The tilted updraft is characteristic of a supercell, which allows the rainfall not to destroy the cell itself ([Atlas,](#)

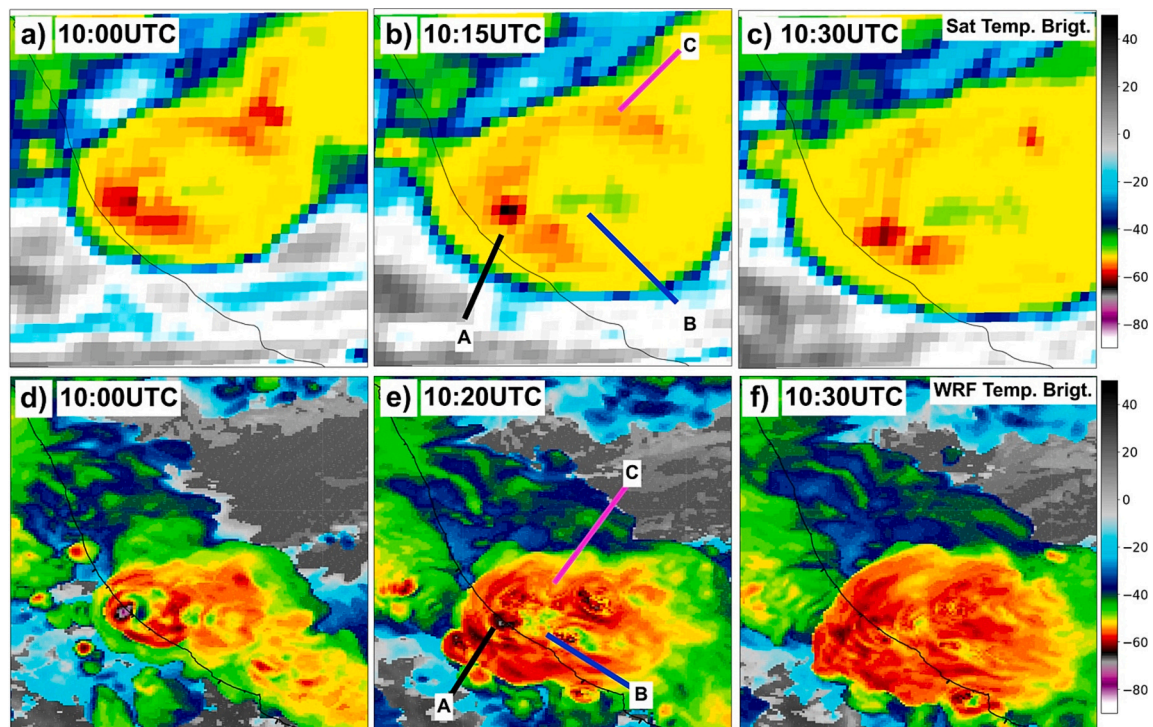
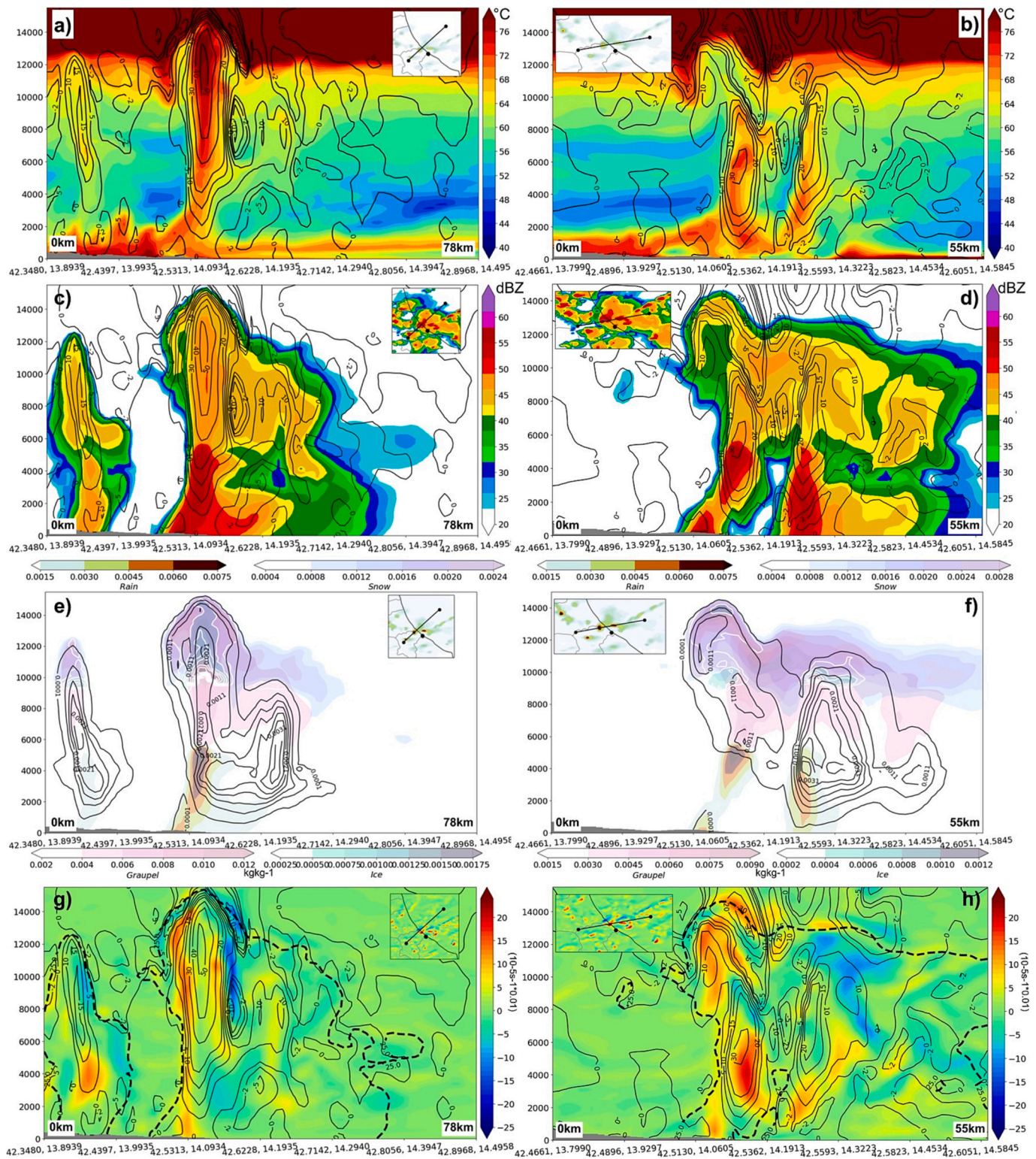


Fig. 6. Panels a-c show the satellite brightness temperature ( $10.8\ \mu\text{m}$ ) every 15 min while the model result is shown in panels d-f every 10 min. Legend: A - overshooting tops, B - Central Warm Spots (CWS), C - cold ring shapes.



**Fig. 7.** The vertical structure of the supercell at 10:10 UTC, shown through the lines shown in the sub-panels. Panels a-b show  $\Theta_e$  ( $^{\circ}\text{C}$ ) and vertical velocity ( $\text{ms}^{-1}$ , contour) values; Panels c-d show vertical speeds and simulated radar reflectivity (dBZ). The cross section of the hydrometeors is shown in panels e-f, dashed colors represent rain ice, snow and graupel, solid lines underline hail (in  $\text{kgkg}^{-1}$ ). Panels g-h show the absolute vorticity ( $10^{-5} \text{ s}^{-1} \cdot 0.01$ ), the vertical velocities (contour) and the 25dBZ value of reflectivity radar (dashed contour).

1966, Nelson, 1983) and eventually to reinforce the cell and to produce hail. This is clearly shown by the increased  $\Theta_e$  (Fig. 7a), due to the latent heating condensation in producing hail and ice (Fig. 7e, solid line and gray color, respectively). As pointed out in the previous section, there was a long-lasting overshooting top associated with a tilted updraft, a

necessary condition for generating giant hailstones (Jurković et al., 2015).

The tilted updraft is clearly shown by the simulated radar reflectivity (Figs. 7c,d) with maximum values of about 55-60dBZ between the surface and 6 km; above these levels the reflectivity decreases to 40-45dBZ